Cell Reports

Article

Vaccine-mediated protection against *Merbecovirus* and *Sarbecovirus* challenge in mice

Graphical abstract

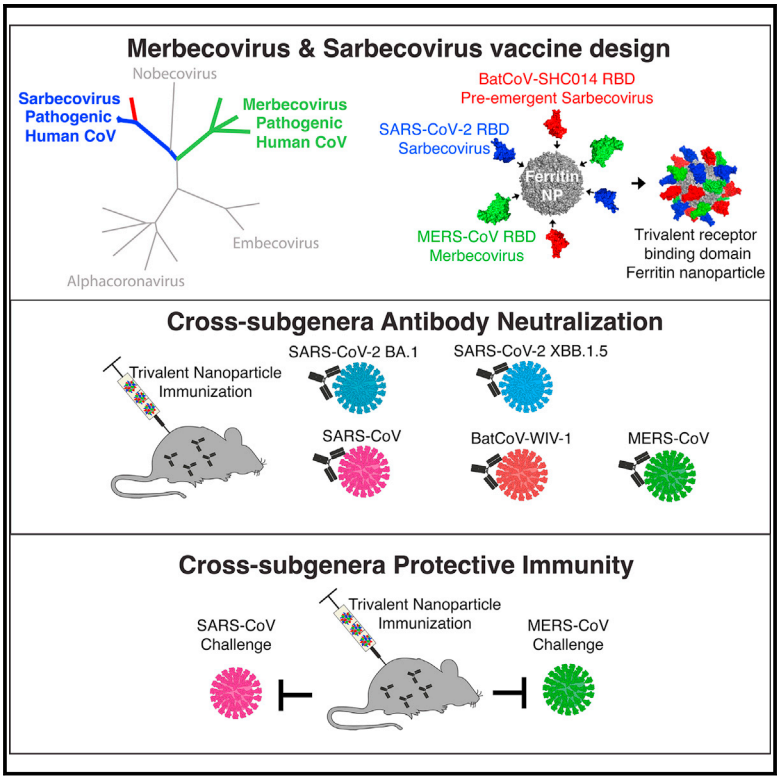

Highlights

- A trivalent RBD nanoparticle vaccine elicits broadly cross-reactive antibodies
- Trivalent RBD nanoparticle vaccine elicits BA.1 and XBB.1.5 neutralizing antibodies
- Vaccine-mediated protection against lethal SARS-CoV and pathogenic MERS-CoV
- A single vaccine protects against group 2b/2c betacoronavirus challenge in mice

Authors

David R. Martinez, Alexandra Schäfer, Tyler D. Gavitt, ..., Ralph S. Baric, Barton F. Haynes, Kevin O. Saunders

Correspondence

david.martinez@yale.edu (D.R.M.), rbaric@email.unc.edu (R.S.B.), barton.haynes@duke.edu (B.F.H.), kevin.saunders@duke.edu (K.O.S.)

In brief

Martinez et al. demonstrate proof of concept that a single ferritin nanoparticle vaccine displaying the receptor-binding domains of MERS-related and SARS-related zoonotic, epidemic, and pandemic coronaviruses elicits broadly cross-reactive binding and neutralizing antibodies against SARS-CoV-2 variants and protects against lethal SARS-CoV and highly pathogenic MERS-CoV disease in mice.

Martinez et al., 2023, Cell Reports ■■, 113248
■■, 2023
https://doi.org/10.1016/j.celrep.2023.113248

CellPress

Please cite this article in press as: Martinez et al., Vaccine-mediated protection against *Merbecovirus* and *Sarbecovirus* challenge in mice, Cell Reports (2023), https://doi.org/10.1016/j.celrep.2023.113248

Cell Reports

CellPress
OPEN ACCESS

Article

Vaccine-mediated protection against *Merbecovirus* and *Sarbecovirus* challenge in mice

David R. Martinez,[1,2,6,7,*] Alexandra Schäfer,[3,6] Tyler D. Gavitt,[4,6] Michael L. Mallory,[3] Esther Lee,[4] Nicholas J. Catanzaro,[3] Haiyan Chen,[4] Kendra Gully,[3] Trevor Scobey,[3] Pooja Koratagere,[4] Alecia Brown,[4] Lena Smith,[4] Robert Parks,[4] Maggie Barr,[4] Amanda Newman,[4] Cindy Bowman,[4] John M. Powers,[3] Erik J. Soderblom,[5] Katayoun Mansouri,[4] Robert J. Edwards,[4] Ralph S. Baric,[3,*] Barton F. Haynes,[4,*] and Kevin O. Saunders[4,*]

[1]Department of Immunobiology, Yale School of Medicine, New Haven, CT 06510, USA
[2]Yale Center for Infection and Immunity, Yale School of Medicine, New Haven, CT 06510, USA
[3]Department of Epidemiology, University of North Carolina at Chapel Hill, Chapel Hill, NC 27599, USA
[4]Duke Human Vaccine Institute, Duke University School of Medicine, Durham, NC 27710, USA
[5]Proteomics and Metabolomics Core Facility, Duke University School of Medicine, Durham, NC 27710, USA
[6]These authors contributed equally
[7]Lead contact
*Correspondence: david.martinez@yale.edu (D.R.M.), rbaric@email.unc.edu (R.S.B.), barton.haynes@duke.edu (B.F.H.), kevin.saunders@duke.edu (K.O.S.)
https://doi.org/10.1016/j.celrep.2023.113248

SUMMARY

The emergence of three highly pathogenic human coronaviruses—severe acute respiratory syndrome coronavirus (SARS-CoV) in 2003, Middle Eastern respiratory syndrome (MERS)-CoV in 2012, and SARS-CoV-2 in 2019—underlines the need to develop broadly active vaccines against the *Merbecovirus* and *Sarbecovirus* betacoronavirus subgenera. While SARS-CoV-2 vaccines protect against severe COVID-19, they do not protect against other sarbecoviruses or merbecoviruses. Here, we vaccinate mice with a trivalent sortase-conjugate nanoparticle (scNP) vaccine containing the SARS-CoV-2, RsSHC014, and MERS-CoV receptor-binding domains (RBDs), which elicited live-virus neutralizing antibody responses. The trivalent RBD scNP elicited serum neutralizing antibodies against bat zoonotic Wuhan Institute of Virology-1 (WIV-1)-CoV, SARS-CoV, SARS-CoV-2 BA.1, SARS-CoV-2 XBB.1.5, and MERS-CoV live viruses. The monovalent SARS-CoV-2 RBD scNP vaccine only protected against *Sarbecovirus* challenge, whereas the trivalent RBD scNP vaccine protected against both *Merbecovirus* and *Sarbecovirus* challenge in highly pathogenic and lethal mouse models. This study demonstrates proof of concept for a single pan-sarbecovirus/pan-merbecovirus vaccine that protects against three highly pathogenic human coronaviruses spanning two betacoronavirus subgenera.

INTRODUCTION

The emergence of severe acute respiratory syndrome coronavirus (SARS-CoV) in 2003, Middle Eastern respiratory syndrome (MERS)-CoV in 2012, and SARS-CoV-2 in 2019 into naive human populations underlines the spillover potential of coronaviruses. SARS-CoV-2 causes coronavirus disease 2019 (COVID-19).[1] The COVID-19 pandemic has had a devastating impact on human health and the world economy. SARS-CoV, SARS-CoV-2, and several zoonotic, pre-emergent SARS- and SARS2-related bat coronaviruses belong to the *Betacoronavirus* genus and the *Sarbecovirus* subgenus and are classified as group 2b coronaviruses.[2–4] Similarly, MERS-CoV and MERS-related bat zoonotic viruses also belong to the *Betacoronavirus* genus and the *Merbecovirus* subgenus and are classified as group 2c coronaviruses.[2,3] Given that in the last two decades, one *Merbecovirus* and two sarbecoviruses have emerged in humans, the development of countermeasures against these important groups of viruses—including universal coronavirus vaccines—is a global health priority.

Several pan-sarbecovirus vaccine approaches have shown early promise in animal models.[5–8] Ferritin sortase-conjugated nanoparticles (scNPs) bearing the SARS-CoV-2 receptor-binding domain (RBD) elicited neutralizing antibodies against bat SARS-related viruses and protected non-human primates (NHPs) against SARS-CoV-2 challenge.[7] Moreover, monovalent SARS-CoV-2 RBD scNP vaccines elicited neutralizing antibodies against all tested SARS-CoV-2 variants including D614G, Beta, Delta, Omicron BA.1, BA.2, BA.2.12.1, and BA.4/BA.5.[9] Similar approaches with RBD NP vaccines also protected against *Sarbecovirus* challenge in mice.[8] RBD NP vaccines and chimeric spike antigens delivered as multiplexed mRNA-lipid nanoparticle (LNP) vaccines similarly protected mice from genetically divergent bat zoonotic SARS-related viruses and SARS-CoV-2 variants.[6,9] Therefore, multiple vaccine designs and modalities have protected against heterologous *Sarbecovirus* challenge in animal models. Importantly, humans infected with SARS-CoV 2003 and/or SARS-CoV-2 generate antibodies capable of neutralizing SARS-related zoonotic viruses and

Please cite this article in press as: Martinez et al., Vaccine-mediated protection against *Merbecovirus* and *Sarbecovirus* challenge in mice, Cell Reports (2023), https://doi.org/10.1016/j.celrep.2023.113248

SARS-CoV-2 variants,[10–14] and monoclonal antibodies (mAbs) isolated from humans protected mice and monkeys from *Sarbecovirus* infection.[10,15] These studies indicated that elicitation of protective neutralizing antibody responses against sarbecoviruses is achievable.

Despite demonstrating proof of principle that vaccines can elicit broad immunity against genetically divergent sarbecoviruses,[5–8,16,17] no study to date has demonstrated vaccine-mediated protection in highly pathogenic/lethal *Sarbecovirus* and *Merbecovirus* challenge animal models. While stem-helix antibodies isolated from humans can protect against group 2b SARS-CoV and SARS-CoV-2 as well as group 2c MERS-CoV in highly pathogenic mouse models,[18] current vaccination strategies do not reproducibly induce immunity targeting these conserved S2 epitopes. Therefore, alternative vaccination strategies that effectively target sarbecoviruses and merbecoviruses are needed.

SARS-CoV-2 spike mRNA vaccines do not protect mice against challenge with genetically divergent zoonotic SARS-related viruses and SARS-CoV.[6] This suggests that currently used SARS-CoV-2 mRNA spike vaccines are unlikely to strongly protect against SARS-related or SARS-CoV-2-related zoonotic viruses or highly evolved SARS-CoV-2 variants of concern that could emerge in the future.[19,20] We therefore developed a trivalent RBD vaccine composed of *Sarbecovirus* and *Merbecovirus* RBDs from zoonotic pre-emergent, human epidemic, and pandemic coronaviruses. In this study, we evaluated the immunogenicity and protective efficacy against SARS-CoV and MERS-CoV in mice. We showed that a monovalent SARS-CoV-2 RBD NP can protect against heterologous *Sarbecovirus* challenge but does not protect against *Merbecovirus* challenge. Conversely, the trivalent RBD scNP generated neutralizing antibodies and prevented severe *Sarbecovirus* disease and *Merbecovirus* infections. This study demonstrates proof of concept in an *in vivo* challenge setting that a single vaccine that protects against both merbecoviruses and sarbecoviruses is an achievable goal.

RESULTS

Generation and validation of trivalent RBD ferritin NP vaccine

We previously reported that a sortase-A-conjugated 24-mer ferritin NP (scNP) monovalent SARS-CoV-2 RBD vaccine elicited broadly neutralizing antibodies against bat zoonotic pre-emergent betacoronaviruses, SARS-CoV, and SARS-CoV-2 variants in NHPs.[7,15] To broaden the response of this SARS-CoV-2 RBD vaccine, we sought to generate a vaccine that increased the immunogenicity against the high-risk *Merbecovirus* (also called group 2c coronavirus) subgenus of betacoronaviruses, which includes MERS-CoV.[2] We designed a trivalent scNP vaccine displaying the SARS-CoV-2 RBD, the SARS-related bat-CoV RsSHC014 RBD, and the MERS-CoV Erasmus Medical Center RBD (Figures 1A and S1A).[9] Equimolar ratios of each RBD were mixed with ferritin to be conjugated to its 24 acceptor sites. Mass spectrometry relative quantification of RBDs conjugated to the assembled NP showed approximately a 1:1:1 conjugation ratio among all three RBDs in the final immunogen (Table S1). In addition to the *Sarbecovirus* SARS-CoV-2 RBD, the RsSHC014 RBD was chosen for inclusion because it is a pre-emergent ACE2-binding *Sarbecovirus*[19] to which the SARS-CoV-2 RBD NP generated only low levels of neutralizing antibodies.[7,15] We used negative-stain electron microscopy (NSEM) to visualize the sortase-A-conjugated trivalent vaccines and demonstrated successful RBD conjugation (Figures 1B and S1B). The trivalent RBD scNP recapitulated the stability of the individual RBDs, indicating that the conjugation reaction had no deleterious effects on RBD folding or stability (Figures S1C and S1D).

To validate the efficient conjugation of SARS-CoV-2/RsSHC014/MERS-CoV RBDs as a trivalent vaccine, we also performed biolayer interferometry (BLI) binding analyses with human monoclonal antibodies that recognize group 2b and 2c coronavirus spike epitopes and human ACE2. The MERS-CoV RBD-specific monoclonal antibodies (mAbs) JC57-14 and CDC-C2 only recognized MERS-CoV spike and the trivalent RBD vaccine (Figure 1C). Similarly, the SARS-CoV-2 RBD-specific mAbs DH1284 and DH1041 bound only to SARS-CoV-2 spike and the trivalent RBD vaccine (Figure 1C). The group 2b RBD cross-reactive mAbs DH1047, DH1235, CR3022, and S309 bound to SARS-CoV-2 spike, RsSHC014 spike, and the trivalent RBD vaccine with the highest magnitude but not to MERS-CoV spike or HIV envelope (Env). Finally, the negative control stem-helix mAb DH1057.1 bound to RsSHC014 spike and SARS-CoV-2 spike but not to the trivalent RBD vaccine, MERS-CoV spike, or HIV Env. Overall, the trivalent RBD scNP bound to all the various group 2b and 2c RBD antibodies, whereas no one spike protein recapitulated this breadth of reactivity. These BLI binding analyses suggest that the trivalent SARS-CoV-2/RsSHC014/MERS-CoV RBD scNP vaccine was efficiently conjugated and that the RBD immunogens are properly recognized by various group 2b- and 2c-reactive mAbs.

Immunogenicity of monovalent versus trivalent scNP vaccines in mice

To compare the immunogenicity of the monovalent versus the trivalent RBD scNP vaccines, we vaccinated aged BALB/c mice two times 4 weeks apart (Figure 2A). The Toll-like receptor 4 agonist glucopyranosyl lipid adjuvant-stable emulsion (GLA-SE) was used as the adjuvant for both vaccine groups and adjuvant-only controls (Figure 2A).[21] We immunized mice with 10 μg of monovalent SARS-CoV-2 RBD scNP vaccine or 10 μg of trivalent SARS-CoV-2/RsSHC014/MERS-CoV RBD scNP vaccine adjuvanted with 5 μg of GLA-SE adjuvant. An additional adjuvant-only group received 5 μg of GLA-SE adjuvant. We measured serum-binding immunoglobulin G (IgG) antibodies against *Sarbecovirus* and *Merbecovirus* spike ectodomain matching the RBDs present in the vaccine and SARS-CoV spike, which was not in the vaccine. In mice vaccinated twice with the SARS-CoV-2/RsSHC014/MERS-CoV trivalent RBD scNP vaccine, high titers of spike-binding IgG antibodies were observed against human outbreak SARS-CoV Tor2 isolate (Figure 2B), bat pre-emergent RsSHC014 (Figure 2C), the SARS-CoV-2 Wuhan-1 outbreak isolate (Figure 2D), and the MERS-CoV EMC isolate (Figure 2E). In agreement with the IgG binding to various group 2b and 2c spikes, we also observed serum antibody blocking of human ACE2 (hACE2) binding to SARS-CoV-2 spike and hDPP4 binding to MERS-CoV in trivalent RBD scNP-vaccinated mice (Figures 2F and 2G). Only the trivalent

Please cite this article in press as: Martinez et al., Vaccine-mediated protection against *Merbecovirus* and *Sarbecovirus* challenge in mice, Cell Reports (2023), https://doi.org/10.1016/j.celrep.2023.113248

CellPress
OPEN ACCESS

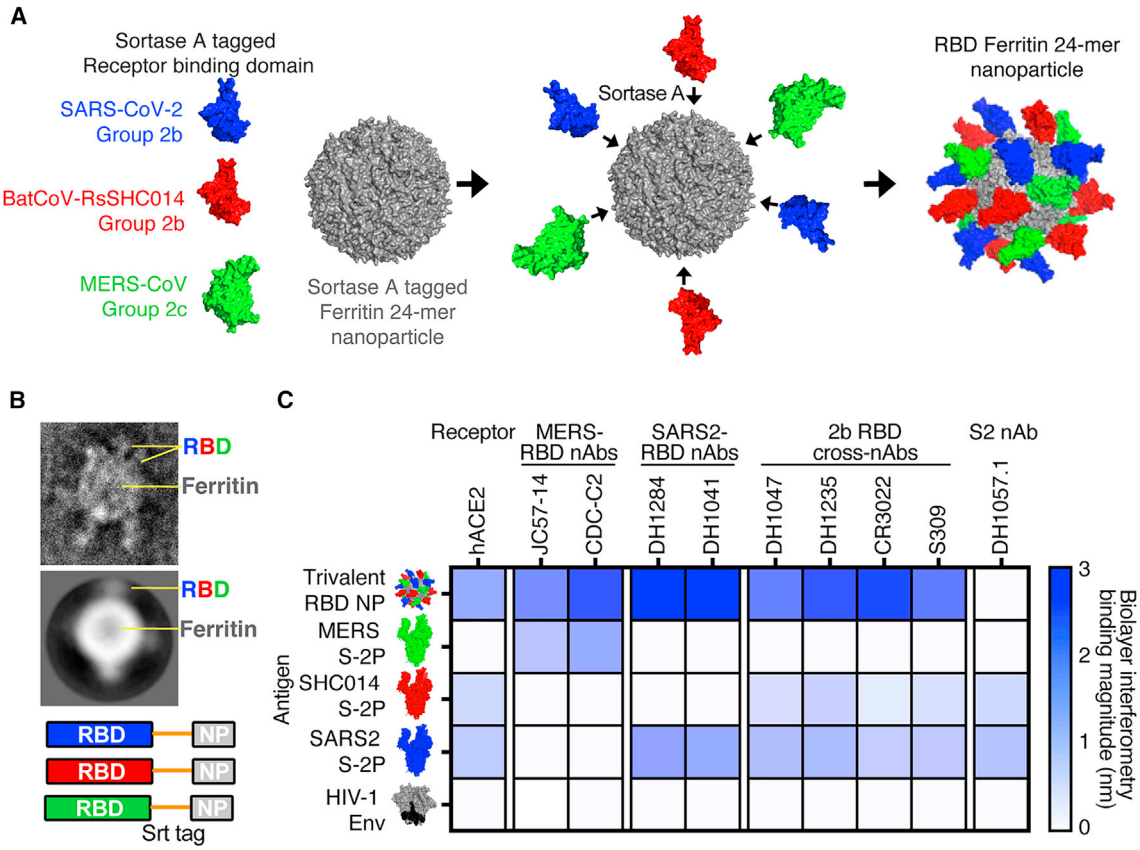

Figure 1. Design and characterization of trivalent RBD scNP vaccines

(A) Ferritin NPs were conjugated with sortase-A-tagged group 2b SARS-CoV-2 RBD, group 2b RsSHC014 RBD, and group 2c MERS-CoV RBD.

(B) Visualization of trivalent scNP was performed via negative-stain electron microscopy.

(C) Validation of trivalent scNP vaccine by biolayer interferometry. Trivalent RBD scNP antigenicity was done by assessing binding of the trivalent vaccine and various group 2b and 2c spikes to hACE2, MERS-CoV RBD mAbs, SARS-CoV-2 RBD mAbs, group 2b cross-reactive RBD mAbs, and an S2 mAb. HIV-1 envelope was included as a negative control antigen.

scNP vaccine elicited robust serum antibody responses capable of blocking hDPP4 (Figure 2G). The monovalent SARS-CoV-2 RBD scNP vaccine also elicited high titers of binding IgG antibodies 2 weeks post-boost against the three *Sarbecovirus* spikes—SARS-CoV Tor2 isolate, RsSHC014, and SARS-CoV-2 Wuhan-1 isolate—and hACE2-blocking antibodies (Figures 2B–2D and 2F). However, immunization with SARS-CoV-2 RBD scNP did not elicit binding IgG to MERS-CoV spike or DPP4-blocking antibodies (Figures 2E and 2G). These data indicated that the monovalent SARS-CoV-2 RBD scNP vaccine elicited cross-reactive binding and serum-blocking antibodies to group 2b, but not group 2c, coronaviruses. Thus, the trivalent RBD scNP vaccine improved antibody responses compared with the monovalent SARS-CoV-2 RBD scNP by eliciting serum antibodies to spikes from all three highly pathogenic human betacoronaviruses and a pre-emergent bat coronavirus.

Induction of SARS-CoV-2 BA.1, XBB.1.5, WIV-1, RsSHC014, and MERS-CoV neutralizing antibodies

We then measured serum neutralizing antibody responses against group 2b and 2c coronaviruses using live-virus assays. At baseline, both the monovalent SARS-CoV-2 RBD and the trivalent SARS-CoV-2/RsSHC014/MERS-CoV RBD scNP-vaccinated mice had undetectable neutralizing antibodies against the highly transmissible SARS-CoV-2 BA.1, SARS-CoV Urbani, and MERS-CoV. Following two immunizations, monovalent SARS-CoV-2 RBD scNP-vaccinated mice elicited serum neutralizing antibodies against SARS-CoV-2 BA.1 with a median inhibitory dilution at which there is an 80% reduction in relative luciferase units (ID_{80}) of 1,832 (Figure 3A). High levels of neutralizing antibodies were raised against WIV-1-CoV with an ID_{80} of 1,165 in the trivalent group and 967 in the monovalent group (Figure 3B). Monovalent-vaccinated mice elicited potent serum neutralizing antibodies against SARS-CoV Urbani with a median ID_{80} of 1,157 (Figure 3C). Undetectable serum neutralizing antibodies were observed against MERS-CoV EMC (Figure 3D). In contrast to the monovalent vaccine, we observed potent serum neutralizing antibodies against MERS-CoV by the trivalent SARS-CoV-2/RsSHC014/MERS-CoV RBD scNP vaccine with a median ID_{80} of 3,424 (Figure 3D). The trivalent SARS-CoV-2/RsSHC014/MERS-CoV RBD scNP vaccine also elicited serum neutralizing antibodies against SARS-CoV-2 BA.1 and SARS-

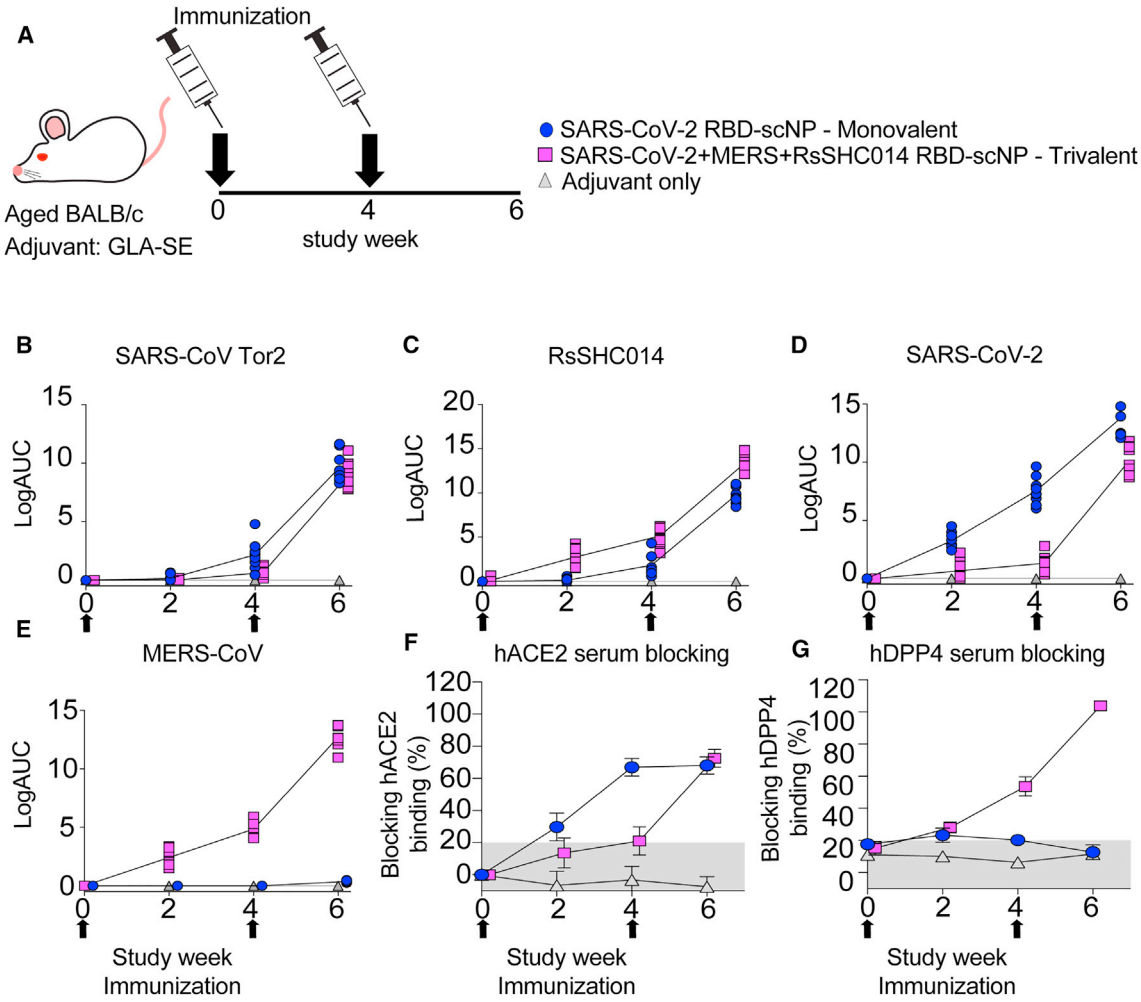

Figure 2. IgG binding responses in mice immunized with monovalent SARS-CoV-2 RBD scNP vaccine, trivalent SARS-CoV-2/RsSHC014/MERS-CoV RBD scNP, and adjuvant alone

(A) BALB/c mice were immunized intramuscularly at weeks 0 and 4 with either monovalent or trivalent vaccines adjuvanted with GLA-SE. Mice were bled 1 day before priming (pre-prime), 1 day before boosting (pre-boost), and 2 weeks post-boost (peak) against the following spike antigens: (B) SARS-CoV Tor2, (C) RsSHC014, (D) SARS-CoV-2, and (E) MERS-CoV.

(F) Vaccine-elicited hACE2-blocking serum responses in monovalent-, trivalent-, and adjuvant-only-vaccinated mice.

(G) Vaccine-elicited hDPP4-blocking serum responses in monovalent-, trivalent-, and adjuvant-only-vaccinated mice. Error bars represent group standard deviation in (F) and (G).

CoV Urbani with ID_{80} values of 251 and 625, respectively. Importantly, undetectable serum neutralizing antibodies were measured in the adjuvant-only-vaccinated mice. Thus, the monovalent SARS-CoV-2 RBD scNP vaccine elicited neutralizing antibodies against pandemic and epidemic sarbecoviruses, whereas trivalent SARS-CoV-2/RsSHC014/MERS-CoV RBD scNP vaccines elicited neutralizing antibodies against pandemic and epidemic sarbecoviruses and MERS-CoV.

Next, we assessed serum neutralization of the widespread, highly resistant SARS-CoV-2 variant XBB.1.5. Modest serum neutralization was observed against SARS-CoV-2 XBB.1.5 in both the monovalent and trivalent vaccine (Figure 4). Five of ten mice immunized three times with either the monovalent RBD scNP or the trivalent SARS-CoV-2/RsSHC014/MERS-CoV RBD scNP vaccine suppressed virus replication by 50% or greater (Figures 4A and 4B). However, only two mice in each group neutralized more than 80% of virus replication, indicating that neutralization was weak. Overall, we observed higher levels of neutralizing antibody titers against SARS-CoV-2 BA.1 and SARS-CoV Urbani as compared with XBB.1.5 (Figure 3).

Protective efficacy of trivalent RBD NP vaccine against group 2b and 2c CoVs

To evaluate the protective efficacy of the trivalent RBD scNP against *Sarbecovirus* and *Merbecovirus* infection with highly pathogenic coronaviruses, we challenged mice with either a heterologous, lethal mouse-adapted SARS-CoV virus (MA15)[22] or a highly pathogenic mouse-adapted MERS-CoV virus (m35c4).[23,24] Aged BALB/c mice immunized with the trivalent SARS-CoV-2/RsSHC014/MERS-CoV RBD scNP were protected

Please cite this article in press as: Martinez et al., Vaccine-mediated protection against *Merbecovirus* and *Sarbecovirus* challenge in mice, Cell Reports (2023), https://doi.org/10.1016/j.celrep.2023.113248

CellPress
OPEN ACCESS

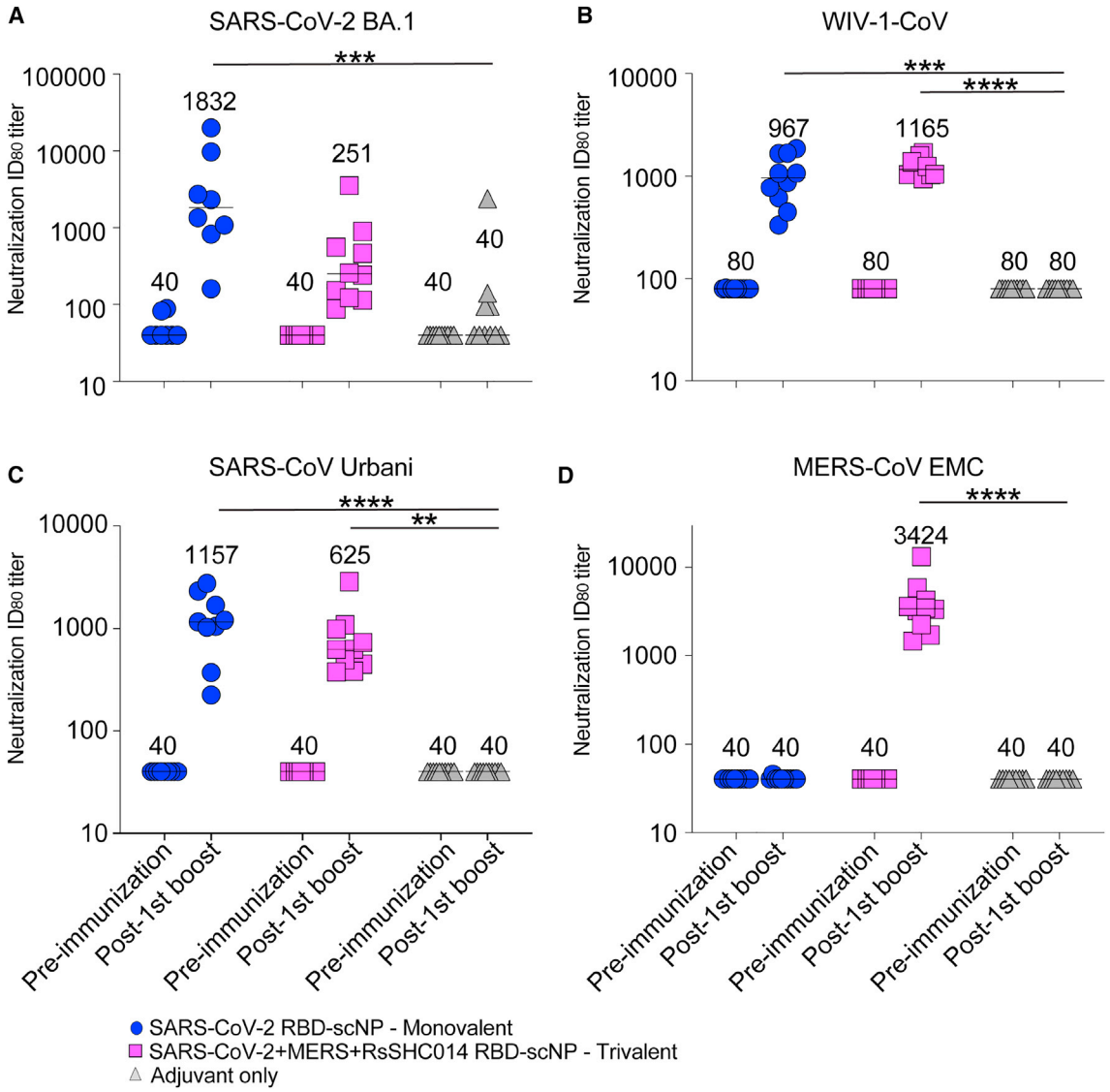

Figure 3. Neutralizing antibodies elicited against group 2b and 2c betacoronaviruses

Live-virus neutralizing activity against (A) SARS-CoV-2 BA.1, (B) bat zoonotic WIV-1-CoV, (C) SARS-CoV Urbani, and (D) MERS-CoV EMC. Mouse sera at baseline and post-boost are shown in 2× vaccinated mice for SARS-CoV-2 BA.1, SARS-CoV Urbani, and MERS-CoV. Mouse sera post second boost were used against WIV-1. Blue circles denote monovalent SARS-CoV-2 RBD scNP-vaccinated mice. Magenta squares denote trivalent SARS-CoV-2/RsSHC014/MERS-CoV RBD scNP-vaccinated mice. Gray triangles denote adjuvant-only control mice. Numerical values in the graphs denote the median ID_{80} values. ID_{80} values are reported as reciprocal serum dilution that inhibits 80% of virus replication. A Kruskal-Wallis non-parametric test with Dunn's multiple comparisons test was used throughout to compare the median ID_{80} values across vaccine groups (*$p < 0.05$, **$p < 0.005$, ***$p < 0.0005$, and ****$p < 0.0001$).

from weight loss (Figure 5A) and mortality (Figure 5B) after SARS-CoV MA15 challenge. This protection was likely due to conserved RBD epitopes shared among sarbecoviruses.[7–9,10] Notably, the monovalent SARS-CoV-2 RBD scNP vaccine also protected against heterologous SARS-CoV MA15 challenge, whereas the adjuvant-only-vaccinated controls had 40% mortality by day 4 post-infection (Figure 5B). Compared with adjuvant-only controls, both monovalent and trivalent RBD scNP-vaccinated mice had reduced lung virus replication at day 2 post-infection as measured by infectious virus plaque assays (Figure 5C). However, only the trivalent scNP-vaccinated mice had lower infectious SARS-CoV replication in the nasal turbinates at day 2 post-infection, as measured by plaque assay, compared with the adjuvant-only-vaccinated controls (Figure 5D). Moreover, the trivalent RBD scNP vaccine also mediated increased protection against upper airway replication of SARS-CoV in mice.

As we observed strong protection from heterologous and highly pathogenic SARS-CoV MA15, we evaluated whether the trivalent vaccine also protected against challenge in a highly pathogenic mouse-adapted MERS-CoV model.[23,24] Like adjuvant-only controls, DPP4 transgenic mice vaccinated twice with a monovalent SARS-CoV-2 RBD scNP vaccine experienced

Please cite this article in press as: Martinez et al., Vaccine-mediated protection against *Merbecovirus* and *Sarbecovirus* challenge in mice, Cell Reports (2023), https://doi.org/10.1016/j.celrep.2023.113248

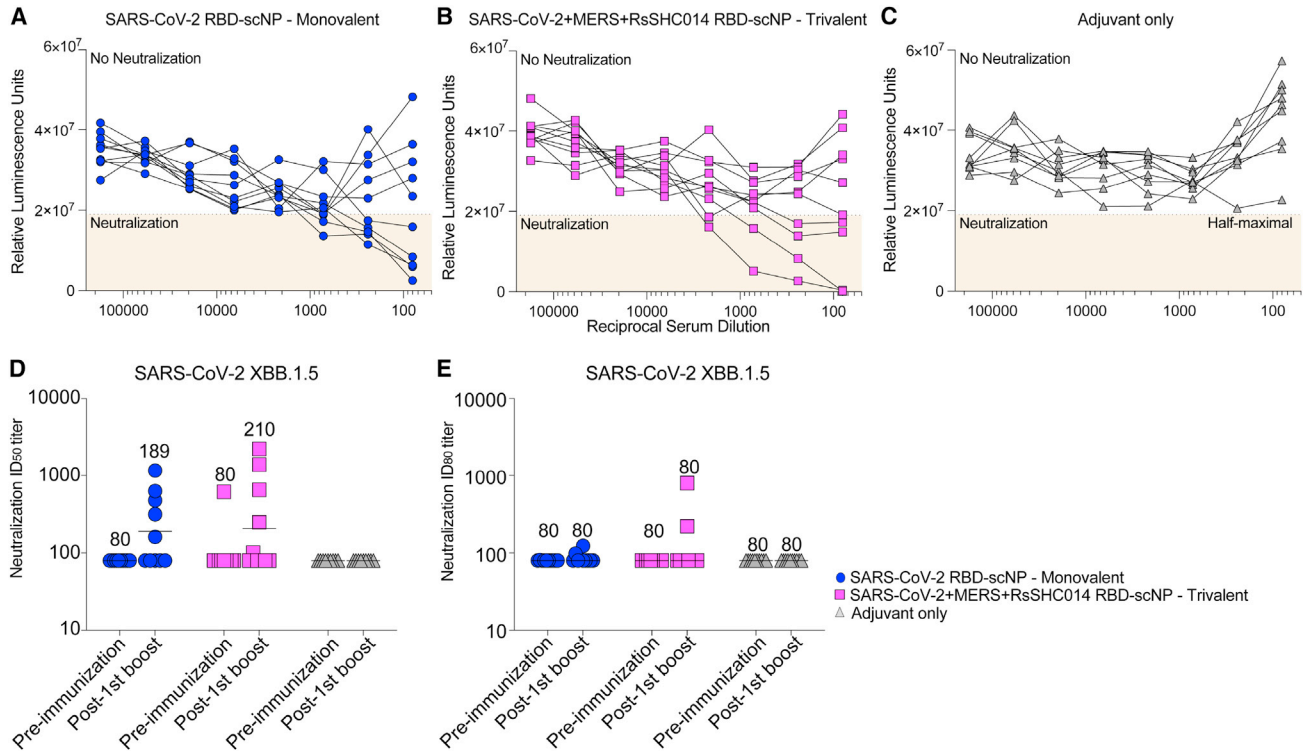

Figure 4. Vaccination of mice with monovalent and trivalent RBD scNP-induced modest neutralization of SARS-CoV-2 XBB1.5 live virus

(A–C) Serum inhibition of virus replication determined by virus reporter luminescence for the (A) monovalent, (B) trivalent, and (C) adjuvant-only vaccines. A reduction in luminescence by more than half of the value seen in control cells that lack serum but are infected is shown as the half-maximal value. Neutralization curves that reach the half-maximal value are considered positive. Each curve shows neutralization by an individual mouse serum sample collected 1 week after the third immunization.

(D and E) The reciprocal dilution of serum required to inhibit (D) 50% or (E) 80% of virus replication. Each symbol represents the value for an individual mouse, with the horizontal bar indicating group geometric mean.

severe MERS-CoV disease including weight loss (Figure S2A) and high levels of infectious virus replication in the lung and nasal turbinates (Figures S2B and S2C). Similarly, by day 4 post-infection, SARS-CoV-2 RBD scNP-vaccinated mice exhibited significant weight loss and high amounts of virus replication in the lung (Figure S2D). In contrast, mice vaccinated twice with the trivalent SARS-CoV-2/RsSHC014/MERS-CoV RBD scNP vaccine were protected from weight loss (Figure S2A). Unlike adjuvant-only controls and SARS-CoV-2 RBD monovalent-vaccinated mice, we observed complete protection from lung virus replication at day 2 post-infection in the 2× trivalent SARS-CoV-2/RsSHC014/MERS-CoV RBD scNP-vaccinated group (Figure S2B). However, we did not observe complete suppression of nasal turbinate MERS-CoV replication at day 2 post-infection and lung virus replication at day 4 post-infection in the 2× trivalent SARS-CoV-2/RsSHC014/MERS-CoV RBD scNP-vaccinated group (Figures S2C and S2D).

To evaluate if additional boosting could increase the protective efficacy in the upper airways of the trivalent SARS-CoV-2/RsSHC014/MERS-CoV RBD scNP vaccine, we repeated the vaccination study in the DPP4-modified mice that are susceptible to MERS-CoV infection and disease. We vaccinated mice three times 4 weeks apart with either the trivalent RBD scNP or the SARS-CoV-2 RBD scNP (Figure S3A). The trivalent SARS-CoV-2/RsSHC014/MERS-CoV RBD scNP vaccine elicited high IgG binding responses against five different group 2b RBDs and four different group 2c RBDs (Figure 6A). In contrast, the monovalent SARS-CoV-2 RBD scNP vaccine only elicited high IgG binding responses to group 2b betacoronaviruses (Figure 6A), demonstrating more limited IgG binding breadth than the trivalent RBD scNP. IgG binding was not observed against group 1, 2a, 2d, or 4 coronaviruses (Figure 6A). Notably, the MERS-CoV RBD in the trivalent vaccine elicited high binding responses against MERS-CoV and HKU5, and markedly lower binding was observed against NL140422 and HKU4 (Figure 6A). This heterogeneous binding across group 2c RBDs suggests that group 2c RBDs may share fewer conserved epitopes as compared to group 2b RBDs (Figure 6A). Notably, mice immunized three times (3×) showed an increase in serum binding IgG against group 2b and 2c coronavirus RBDs compared with mice immunized twice, indicating that the additional boost augmented antibody responses (Figure S3B).

Three immunizations with the trivalent SARS-CoV-2/RsSHC014/MERS-CoV RBD scNP vaccine completely protected mice from weight loss (Figure 6B), and lung virus replication at days 3 and 5 following MERS-CoV challenge (Figures 6C and 6E). Importantly, mice vaccinated 3× with the trivalent vaccine were fully protected from MERS-CoV replication in the nasal

Please cite this article in press as: Martinez et al., Vaccine-mediated protection against *Merbecovirus* and *Sarbecovirus* challenge in mice, Cell Reports (2023), https://doi.org/10.1016/j.celrep.2023.113248

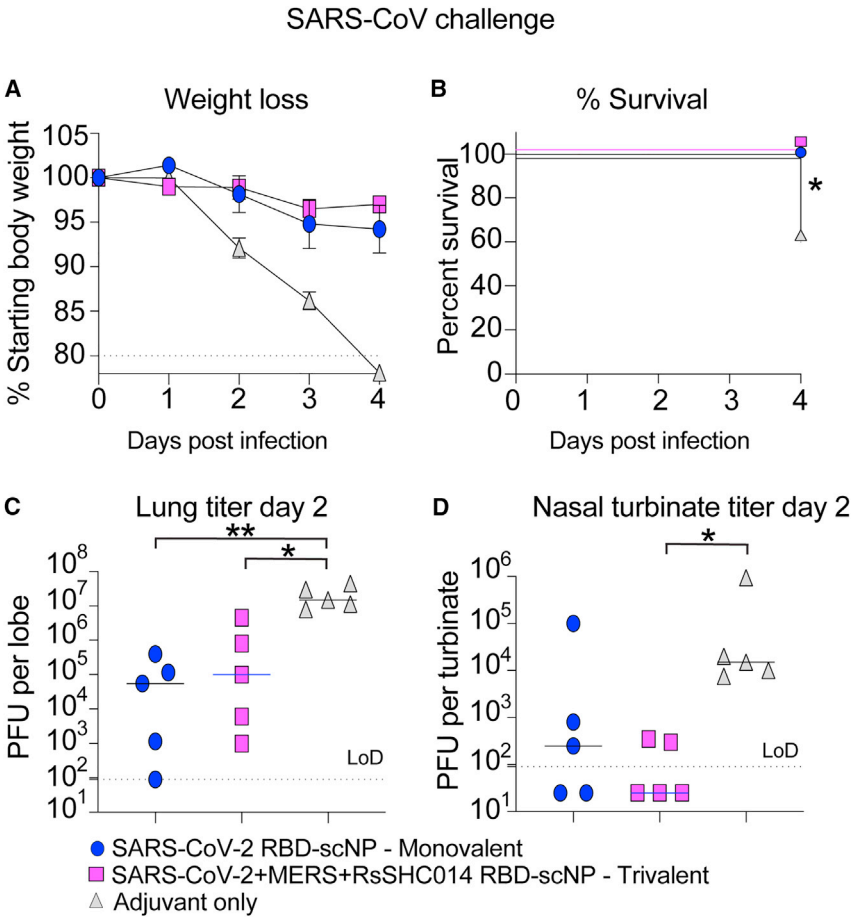

Figure 5. Protective efficacy of monovalent versus trivalent RBD scNP vaccines against SARS-CoV challenge in mice

(A) Weight loss in monovalent SARS-CoV-2 RBD scNP-, trivalent SARS-CoV-2/RsSHC014/MERS-CoV RBD scNP-, and adjuvant-only-vaccinated mice. Error bars represent SEM.

(B) Percentage of survival in vaccinated mice versus control mice following lethal SARS-CoV Urbani MA15 challenge. Statistical significance of the survival curves is from a chi-squared log-rank test.

(C) Infectious virus replication (plaque forming units: PFU) in the lung of vaccinated mice at day 2 following infection. Statistical significance is from a Kruskal-Wallis test following a Dunn's multiple comparison correction test.

(D) Infectious virus replication in nasal turbinates at day 2 post-infection. Statistical significance is from a Kruskal-Wallis test following a Dunn's multiple comparison correction test. Blue circles represent the monovalent-vaccinated mice. Magenta squares represent the trivalent-vaccinated mice. Gray triangles denote the adjuvant-only-vaccinated mice. *p < 0.05, **p < 0.005, ***p < 0.0005, and ****p < 0.0001.

turbinates (Figure 6D). In contrast, the adjuvant-only control and the SARS-CoV-2 RBD monovalent scNP vaccine group exhibited marked weight loss following MERS-CoV challenge (Figure 6B) and had high levels of virus replication in the lungs and nasal turbinates at day 3 (Figures 6C and 6D). At day 5 post-infection, virus replication remained high in these two groups of mice (Figure 6E). Overall, both MERS-CoV challenge studies demonstrated protection in the trivalent NP vaccine group (Figures 6 and S2). In both the 2× and 3× vaccination studies, we observed protection from weight loss, and complete protection was observed from lung virus replication in the early time point (Figures 6B, 6C, S2A, and S2B). However, we only observed complete protection from upper airway and lung replication at later time points in the trivalent vaccine group vaccinated 3× (Figures 6D, 6E, S2C, and S2D). Therefore, a three-dose vaccination strategy achieved a high degree of protection in both the lower and upper airways after challenge with MERS-CoV.

DISCUSSION

Given the more than 6.8 million deaths attributed to the SARS-CoV-2 pandemic, vaccines that protect against the known highly pathogenic human coronaviruses are needed.[25,26] While previous studies demonstrated that other NPs[8] and multivalent nanoscaffolds[27] can elicit immunogenic responses and protect against SARS-CoV-2 and variants, our ferritin scNP trivalent vaccine is the first to demonstrate proof of concept that protection against group 2b and 2c highly pathogenic human coronaviruses is achievable *in vivo*. This current study demonstrated that a trivalent RBD scNP vaccine induced neutralizing antibodies against all three highly pathogenic human betacoronaviruses and protected against both heterologous group 2b (*Sarbecovirus* subgenus) and homologous group 2c (*Merbecovirus* subgenus) coronavirus infections. This vaccine is an advance over current SARS-CoV-2 mRNA vaccines, which lack protection against other human pathogenic betacoronaviruses such as SARS-CoV and MERS-CoV.[6] The trivalent vaccine is also an advance beyond current group 2b-focused RBD NP vaccines. The monovalent SARS-CoV-2 RBD scNP vaccine used in this study elicited high concentrations of IgG antibodies against group 2b RBDs and, in previous studies, was shown to neutralize recent known SARS-CoV-2 variants including highly mutated BA.4/BA.5 Omicron substrains.[9] Moreover, the monovalent SARS-CoV-2 RBD scNP vaccine protects against sarbecoviruses SARS-CoV, SARS-CoV-2, and RsSHC014.[9] However, this SARS-CoV-2 RBD NP did not generate cross-reactive antibodies against group 2c spike.[7] Notably, monovalent scNP SARS-CoV-2 vaccines that protect mice and monkeys against SARS-CoV-2 and *Sarbecovirus* challenge[7,9] did not protect against MERS-CoV challenge. The lack of broadly reactive group 2b and 2c antibodies is expected given that MERS-CoV and SARS-CoV-2 RBDs differ in overall structure.[28,29] Therefore, "universal" vaccine approaches targeting SARS-CoV-2 variants may be distinct

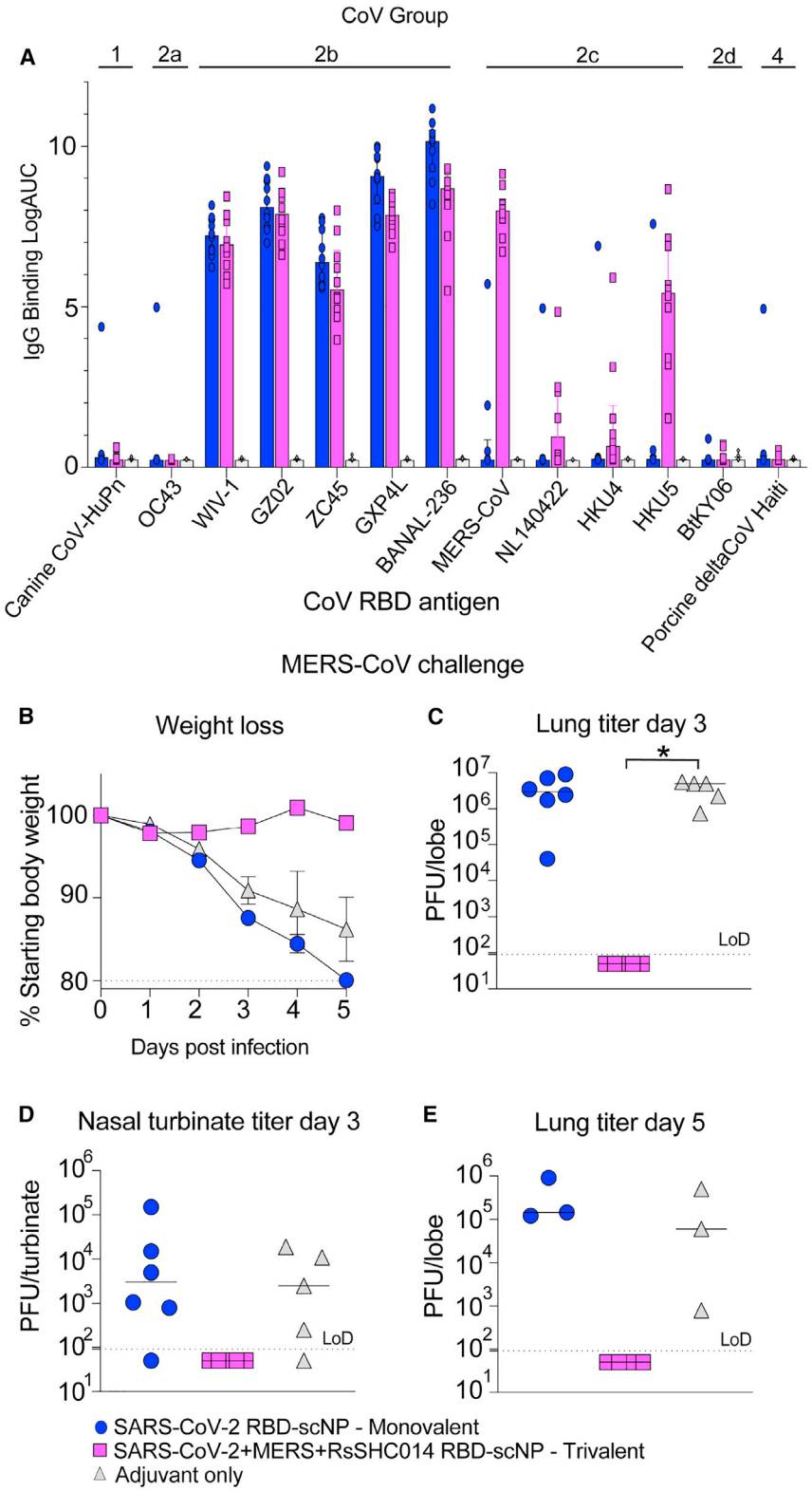

Figure 6. Protective efficacy of monovalent versus trivalent RBD scNP vaccines against MERS-CoV challenge in mice

(A) Cross-reactivity of monovalent and trivalent versus adjuvant-only IgG responses at 1 week post-second boost (peak) against group 1 (canine CoV-HuPn); 2a (OC43); 2b (WIV-1, SARS-CoV GZ02, ZC45, GXP4L, and BANAL-236); 2c (MERS-CoV, NL140422, HKU4, and HKU5); 2d (BtKY06); and 4 (porcine DeltaCoV Haiti) coronavirus RBDs. Bars indicate the group median, and error bars indicate the interquartile range.

(B) Weight loss in SARS-CoV-2 RBD monovalent-, SARS-CoV-2/RsSHC014/MERS-CoV RBD scNP-, and adjuvant-only-vaccinated mice following MERS-CoV intranasal challenge. Error bars represent SEM.

(C) Lung virus replication in monovalent, trivalent, and adjuvant-only controls at day 3 post-infection.

(D) Infectious virus replication in nasal turbinates at day 3 post-infection.

(E) Lung infectious virus replication at day 5 post infection.

p values shown are from a Kruskal-Wallis test following a Dunn's multiple comparisons test. *$p < 0.05$, **$p < 0.005$, ***$p < 0.0005$, and ****$p < 0.0001$.

from those approaches needed for vaccines against antigenically and genetically distant coronaviruses.

Importantly, the SARS-CoV-2 RBD was sufficient in the monovalent vaccine for eliciting cross-reactive IgG antibodies against all tested sarbecoviruses. To bolster immunity against sarbecoviruses, the trivalent RBD scNP includes the SHC014 RBD. Conversely, the MERS-CoV RBD in the trivalent RBD vaccine elicited a range of high and low binding IgG titers to the four group 2c RBDs tested. The inability of a single group 2c RBD to elicit high titers of cross-reactive IgG to all group 2c RBDs tested indicates that group 2c RBDs may share less epitope conservation compared with group 2b RBDs.

The development of MERS-CoV vaccines designed to elicit high titer antibody responses has been of concern given reports that antibody dependent enhancement of infection can occur *in vitro* with MERS-CoV-reactive antibodies.[30] Increased virus replication that is mediated by IgG antibodies is a classical surrogate of antibody-dependent enhancement that is observed for flaviviruses like dengue virus.[31] In our study, we observed potent serum antibody neutralization of MERS-CoV *in vitro* and no evidence of increased virus replication upon challenge of mice immunized with the MERS-CoV RBD. It is also important to note that we did not observe increased lung or nasal turbinate MERS-CoV replication relative to adjuvant-only controls in mice vaccinated with the monovalent SARS-CoV-2 RBD scNP vaccine, even though this vaccine did not protect against MERS-CoV challenge. This is an important observation, as it suggests that individuals that have SARS-CoV-2 immunity to the RBD are unlikely to experience more severe disease when exposed to MERS-CoV or to a distinct group 2c coronavirus that is antigenically like MERS-CoV.

Finally, our study shows the utility of the scNP platform for rapidly and easily generating broadly protective vaccines. The trivalent RBD scNP vaccine is a viable strategy for vaccine-mediated protection against the three highly pathogenic group 2b and 2c betacoronaviruses—SARS-CoV, SARS-CoV-2 and its variants, and MERS-CoV. Moving forward, it will be critical to assess if this trivalent RBD scNP vaccine also protects against group 2b and 2c coronaviruses in additional mouse models that express hACE2 in the upper and lower airway epithelium, as is observed in humans[32] and in other MERS-CoV mouse challenge models.[33]

Limitations of the study

A limitation to our study is that mucosal antibody responses were not measured. Thus, the durability of vaccine-elicited neutralizing antibodies in the upper airway is not known. Similarly, tissue-resident memory B and T cells responses were not profiled in the nasal airways or the lungs.[16] Another limitation to our study is that the group 2c challenge was homologous to the MERS-CoV RBD in the trivalent scNP vaccine. However, this is currently a limitation of the broad coronavirus pathogenesis field, as MERS-CoV is the only currently known group 2c human respiratory coronavirus that can replicate and cause disease in mice expressing humanized DPP4 receptors. Our study also indicates that careful consideration must be given to the number of unique antigens conjugated to the NP, as adding too many divergent RBDs may dilute the potent immunogenicity of any one RBD. The need for a second or third boost of trivalent RBD scNP in our studies may be indicative of this point. Altogether, our results suggest that universal vaccine approaches targeting group 2b and 2c coronaviruses are achievable via multivalent delivery of RBDs via adjuvanted NP vaccines. The protective group 2c immunity generated by the trivalent RBD scNP is important since previous MERS-CoV outbreaks have had case fatality rates as high as 40%,[34] far exceeding the 1%–10% rate reported for SARS-CoV-2 and SARS-CoV.[35] The next generation of coronavirus vaccines will need to broaden protection to include both group 2b and 2c coronaviruses. Additionally, these findings have important implications for slowing down or preventing the spread of pre-emergent, zoonotic coronaviruses poised for human emergence.[19,20,36]

STAR★METHODS

Detailed methods are provided in the online version of this paper and include the following:

- KEY RESOURCES TABLE
- RESOURCE AVAILABILITY
  - Lead contact
  - Materials availability
  - Data and code availability
- EXPERIMENTAL MODEL AND STUDY PARTICIPANT DETAILS
  - Mouse models
- METHOD DETAILS
  - Recombinant protein production
- RBD SORTASE A CONJUGATED NANOPARTICLE VACCINE PRODUCTION
  - LC-MS/MS proteomics analysis
  - Biolayer interferometry (BLI)
  - Negative stain electron microscopy of RBD nanoparticles
  - Processing of negative-stain images
  - Mouse vaccinations and virus challenge experiments
  - Binding ELISA against coronavirus antigen panel
  - ACE2-blocking and DPP4-blocking assays
  - Live virus neutralization assays
  - Biocontainment and biosafety
- QUANTIFICATION AND STATISTICAL ANALYSIS

SUPPLEMENTAL INFORMATION

Supplemental information can be found online at https://doi.org/10.1016/j.celrep.2023.113248.

ACKNOWLEDGMENTS

D.R.M. is supported by a Hanna H. Gray Fellowship from the Howard Hughes Medical Institute. This project was supported by the NIAID, NIH, US Department of Health and Human Services award U54 CA260543 (to R.S.B.) and P01 AI158571 (to B.F.H.), as well as an animal model contract from the NIH (HHSN272201700036I).

AUTHOR CONTRIBUTIONS

D.R.M., R.S.B., B.F.H., and K.O.S. conceived the study. D.R.M., T.D.G., A.S., R.S.B., B.F.H., and K.O.S. designed experiments. D.R.M., T.D.G., A.S., M.L.M., N.J.C., K.G., T.S., R.J.E., and K.M. performed laboratory experiments. D.R.M., T.D.G., A.S., M.L.M., N.J.C., K.G., T.S., R.S.B., B.F.H., and K.O.S. analyzed the data and provided critical insight. D.R.M. wrote the first draft of the paper. D.R.M., T.D.G., A.S., M.L.M., N.J.C., K.G., T.S., R.S.B., B.F.H., and K.O.S. edited the paper. All authors read and approved the final version of the paper.

DECLARATION OF INTERESTS

B.F.H. and K.O.S. have filed US patents regarding the nanoparticle vaccine. R.S.B. is on the scientific advisory boards of VaxArt, Invivyd, and Takeda.

INCLUSION AND DIVERSITY

One or more of the authors of this paper self-identifies as an underrepresented ethnic minority in their field of research or within their geographical location. One or more of the authors of this paper self-identifies as a member of the LGBTQIA+ community. One or more of the authors of this paper received support from a program designed to increase minority representation in their field of research.

Received: May 2, 2023
Revised: August 30, 2023
Accepted: September 26, 2023
Published: October 18, 2023

REFERENCES

1. Zhu, N., Zhang, D., Wang, W., Li, X., Yang, B., Song, J., Zhao, X., Huang, B., Shi, W., Lu, R., et al. (2020). A Novel Coronavirus from Patients with Pneumonia in China, 2019. N. Engl. J. Med. *382*, 727–733. https://doi.org/10.1056/NEJMoa2001017.
2. Cui, J., Li, F., and Shi, Z.L. (2019). Origin and evolution of pathogenic coronaviruses. Nat. Rev. Microbiol. *17*, 181–192. https://doi.org/10.1038/s41579-018-0118-9.
3. Graham, R.L., Donaldson, E.F., and Baric, R.S. (2013). A decade after SARS: strategies for controlling emerging coronaviruses. Nat. Rev. Microbiol. *11*, 836–848. https://doi.org/10.1038/nrmicro3143.
4. Coronaviridae Study Group of the International Committee on Taxonomy of Viruses (2020). The species *Severe acute respiratory syndrome-related coronavirus*: classifying 2019-nCoV and naming it SARS-CoV-2. Nat. Microbiol. *5*, 536–544. https://doi.org/10.1038/s41564-020-0695-z.
5. Cohen, A.A., Gnanapragasam, P.N.P., Lee, Y.E., Hoffman, P.R., Ou, S., Kakutani, L.M., Keeffe, J.R., Wu, H.-J., Howarth, M., West, A.P., et al. (2021). Mosaic nanoparticles elicit cross-reactive immune responses to zoonotic coronaviruses in mice. Science *371*, 735–741. https://doi.org/10.1126/science.abf6840.
6. Martinez, D.R., Schäfer, A., Leist, S.R., De la Cruz, G., West, A., Atochina-Vasserman, E.N., Lindesmith, L.C., Pardi, N., Parks, R., Barr, M., et al. (2021). Chimeric spike mRNA vaccines protect against Sarbecovirus challenge in mice. Science *373*, 991–998. https://doi.org/10.1126/science.abi4506.
7. Saunders, K.O., Lee, E., Parks, R., Martinez, D.R., Li, D., Chen, H., Edwards, R.J., Gobeil, S., Barr, M., Mansouri, K., et al. (2021). Neutralizing antibody vaccine for pandemic and pre-emergent coronaviruses. Nature *594*, 553–559. https://doi.org/10.1038/s41586-021-03594-0.
8. Walls, A.C., Miranda, M.C., Schäfer, A., Pham, M.N., Greaney, A., Arunachalam, P.S., Navarro, M.-J., Tortorici, M.A., Rogers, K., O'Connor, M.A., et al. (2021). Elicitation of broadly protective sarbecovirus immunity by receptor-binding domain nanoparticle vaccines. Cell *184*, 5432–5447.e16. https://doi.org/10.1016/j.cell.2021.09.015.
9. Li, D., Martinez, D.R., Schäfer, A., Chen, H., Barr, M., Sutherland, L.L., Lee, E., Parks, R., Mielke, D., Edwards, W., et al. (2022). Breadth of SARS-CoV-2 neutralization and protection induced by a nanoparticle vaccine. Nat. Commun. *13*, 6309. https://doi.org/10.1038/s41467-022-33985-4.
10. Martinez, D.R., Schäfer, A., Gobeil, S., Li, D., De la Cruz, G., Parks, R., Lu, X., Barr, M., Stalls, V., Janowska, K., et al. (2022). A broadly cross-reactive antibody neutralizes and protects against sarbecovirus challenge in mice. Sci. Transl. Med. *14*, eabj7125. https://doi.org/10.1126/scitranslmed.abj7125.
11. Pinto, D., Park, Y.-J., Beltramello, M., Walls, A.C., Tortorici, M.A., Bianchi, S., Jaconi, S., Culap, K., Zatta, F., De Marco, A., et al. (2020). Cross-neutralization of SARS-CoV-2 by a human monoclonal SARS-CoV antibody. Nature *583*, 290–295. https://doi.org/10.1038/s41586-020-2349-y.
12. Rappazzo, C.G., Tse, L.V., Kaku, C.I., Wrapp, D., Sakharkar, M., Huang, D., Deveau, L.M., Yockachonis, T.J., Herbert, A.S., Battles, M.B., et al. (2021). Broad and potent activity against SARS-like viruses by an engineered human monoclonal antibody. Science *371*, 823–829. https://doi.org/10.1126/science.abf4830.
13. He, W.T., Musharrafieh, R., Song, G., Dueker, K., Tse, L.V., Martinez, D.R., Schäfer, A., Callaghan, S., Yong, P., Beutler, N., et al. (2022). Targeted isolation of diverse human protective broadly neutralizing antibodies against SARS-like viruses. Nat. Immunol. *23*, 960–970. https://doi.org/10.1038/s41590-022-01222-1.
14. Tan, C.W., Chia, W.N., Young, B.E., Zhu, F., Lim, B.L., Sia, W.R., Thein, T.L., Chen, M.I.C., Leo, Y.S., Lye, D.C., and Wang, L.F. (2021). Pan-Sarbecovirus Neutralizing Antibodies in BNT162b2-Immunized SARS-CoV-1 Survivors. N. Engl. J. Med. *385*, 1401–1406. https://doi.org/10.1056/NEJMoa2108453.
15. Li, D., Edwards, R.J., Manne, K., Martinez, D.R., Schäfer, A., Alam, S.M., Wiehe, K., Lu, X., Parks, R., Sutherland, L.L., et al. (2021). In vitro and in vivo functions of SARS-CoV-2 infection-enhancing and neutralizing antibodies. Cell *184*, 4203–4219.e32. https://doi.org/10.1016/j.cell.2021.06.021.
16. Mao, T., Israelow, B., Peña-Hernández, M.A., Suberi, A., Zhou, L., Luyten, S., Reschke, M., Dong, H., Homer, R.J., Saltzman, W.M., and Iwasaki, A. (2022). Unadjuvanted intranasal spike vaccine elicits protective mucosal immunity against sarbecoviruses. Science *378*, eabo2523. https://doi.org/10.1126/science.abo2523.
17. Peng, L., Fang, Z., Renauer, P.A., McNamara, A., Park, J.J., Lin, Q., Zhou, X., Dong, M.B., Zhu, B., Zhao, H., et al. (2022). Multiplexed LNP-mRNA vaccination against pathogenic coronavirus species. Cell Rep. *40*, 111160. https://doi.org/10.1016/j.celrep.2022.111160.
18. Zhou, P., Song, G., Liu, H., Yuan, M., He, W.T., Beutler, N., Zhu, X., Tse, L.V., Martinez, D.R., Schäfer, A., et al. (2023). Broadly neutralizing anti-S2 antibodies protect against all three human betacoronaviruses that cause deadly disease. Immunity *56*, 669–686.e7. https://doi.org/10.1016/j.immuni.2023.02.005.
19. Menachery, V.D., Yount, B.L., Jr., Debbink, K., Agnihothram, S., Gralinski, L.E., Plante, J.A., Graham, R.L., Scobey, T., Ge, X.Y., Donaldson, E.F., et al. (2015). A SARS-like cluster of circulating bat coronaviruses shows potential for human emergence. Nat. Med. *21*, 1508–1513. https://doi.org/10.1038/nm.3985.
20. Menachery, V.D., Yount, B.L., Jr., Sims, A.C., Debbink, K., Agnihothram, S.S., Gralinski, L.E., Graham, R.L., Scobey, T., Plante, J.A., Royal, S.R., et al. (2016). SARS-like WIV1-CoV poised for human emergence. Proc. Natl. Acad. Sci. USA. *113*, 3048–3053. https://doi.org/10.1073/pnas.1517719113.
21. Behzad, H., Huckriede, A.L.W., Haynes, L., Gentleman, B., Coyle, K., Wilschut, J.C., Kollmann, T.R., Reed, S.G., and McElhaney, J.E. (2012). GLA-SE, a synthetic toll-like receptor 4 agonist, enhances T-cell responses to influenza vaccine in older adults. J. Infect. Dis. *205*, 466–473. https://doi.org/10.1093/infdis/jir769.
22. Roberts, A., Deming, D., Paddock, C.D., Cheng, A., Yount, B., Vogel, L., Herman, B.D., Sheahan, T., Heise, M., Genrich, G.L., et al. (2007). A

mouse-adapted SARS-coronavirus causes disease and mortality in BALB/c mice. PLoS Pathog. *3*, e5. https://doi.org/10.1371/journal.ppat.0030005.

23. Cockrell, A.S., Yount, B.L., Scobey, T., Jensen, K., Douglas, M., Beall, A., Tang, X.C., Marasco, W.A., Heise, M.T., and Baric, R.S. (2016). A mouse model for MERS coronavirus-induced acute respiratory distress syndrome. Nat. Microbiol. *2*, 16226. https://doi.org/10.1038/nmicrobiol.2016.226.
24. Douglas, M.G., Kocher, J.F., Scobey, T., Baric, R.S., and Cockrell, A.S. (2018). Adaptive evolution influences the infectious dose of MERS-CoV necessary to achieve severe respiratory disease. Virology *517*, 98–107. https://doi.org/10.1016/j.virol.2017.12.006.
25. Burton, D.R., and Walker, L.M. (2020). Rational Vaccine Design in the Time of COVID-19. Cell Host Microbe *27*, 695–698. https://doi.org/10.1016/j.chom.2020.04.022.
26. Dolgin, E. (2022). Pan-coronavirus vaccine pipeline takes form. Nat. Rev. Drug Discov. *21*, 324–326. https://doi.org/10.1038/d41573-022-00074-6.
27. Halfmann, P.J., Castro, A., Loeffler, K., Frey, S.J., Chiba, S., Kawaoka, Y., and Kane, R.S. (2021). Potent neutralization of SARS-CoV-2 including variants of concern by vaccines presenting the receptor-binding domain multivalently from nanoscaffolds. Bioeng. Transl. Med. *6*, e10253. https://doi.org/10.1002/btm2.10253.
28. Wang, N., Shi, X., Jiang, L., Zhang, S., Wang, D., Tong, P., Guo, D., Fu, L., Cui, Y., Liu, X., et al. (2013). Structure of MERS-CoV spike receptor-binding domain complexed with human receptor DPP4. Cell Res. *23*, 986–993. https://doi.org/10.1038/cr.2013.92.
29. Huo, J., Zhao, Y., Ren, J., Zhou, D., Duyvesteyn, H.M.E., Ginn, H.M., Carrique, L., Malinauskas, T., Ruza, R.R., Shah, P.N.M., et al. (2020). Neutralization of SARS-CoV-2 by Destruction of the Prefusion Spike. Cell Host Microbe *28*, 445–454.e6. https://doi.org/10.1016/j.chom.2020.06.010.
30. Wan, Y., Shang, J., Sun, S., Tai, W., Chen, J., Geng, Q., He, L., Chen, Y., Wu, J., Shi, Z., et al. (2020). Molecular Mechanism for Antibody-Dependent Enhancement of Coronavirus Entry. J. Virol. *94*, e02015-19. https://doi.org/10.1128/jvi.02015-19.
31. Martinez, D.R., Metz, S.W., and Baric, R.S. (2021). Dengue Vaccines: The Promise and Pitfalls of Antibody-Mediated Protection. Cell Host Microbe *29*, 13–22. https://doi.org/10.1016/j.chom.2020.12.011.
32. Snouwaert, J.N., Jania, L.A., Nguyen, T., Martinez, D.R., Schäfer, A., Catanzaro, N.J., Gully, K.L., Baric, R.S., Heise, M., Ferris, M.T., et al. (2023). Human ACE2 expression, a major tropism determinant for SARS-CoV-2, is regulated by upstream and intragenic elements. PLoS Pathog. *19*, e1011168. https://doi.org/10.1371/journal.ppat.1011168.
33. Li, K., Wohlford-Lenane, C.L., Channappanavar, R., Park, J.E., Earnest, J.T., Bair, T.B., Bates, A.M., Brogden, K.A., Flaherty, H.A., Gallagher, T., et al. (2017). Mouse-adapted MERS coronavirus causes lethal lung disease in human DPP4 knockin mice. Proc. Natl. Acad. Sci. USA. *114*, E3119–E3128. https://doi.org/10.1073/pnas.1619109114.
34. Zumla, A., Hui, D.S., and Perlman, S. (2015). Middle East respiratory syndrome. Lancet *386*, 995–1007. https://doi.org/10.1016/s0140-6736(15)60454-8.
35. Cao, Y., Hiyoshi, A., and Montgomery, S. (2020). COVID-19 case-fatality rate and demographic and socioeconomic influencers: worldwide spatial regression analysis based on country-level data. BMJ Open *10*, e043560. https://doi.org/10.1136/bmjopen-2020-043560.
36. Hou, Y.J., Chiba, S., Leist, S.R., Meganck, R.M., Martinez, D.R., Schäfer, A., Catanzaro, N.J., Sontake, V., West, A., Edwards, C.E., et al. (2023). Host range, transmissibility and antigenicity of a pangolin coronavirus. Nat. Microbiol. *8*, 1820–1833. https://doi.org/10.1038/s41564-023-01476-x.
37. Hou, Y.J., Okuda, K., Edwards, C.E., Martinez, D.R., Asakura, T., Dinnon, K.H., 3rd, Kato, T., Lee, R.E., Yount, B.L., Mascenik, T.M., et al. (2020). SARS-CoV-2 Reverse Genetics Reveals a Variable Infection Gradient in the Respiratory Tract. Cell *182*, 429–446.e14. https://doi.org/10.1016/j.cell.2020.05.042.
38. Sheahan, T.P., Sims, A.C., Graham, R.L., Menachery, V.D., Gralinski, L.E., Case, J.B., Leist, S.R., Pyrc, K., Feng, J.Y., Trantcheva, I., et al. (2017). Broad-spectrum antiviral GS-5734 inhibits both epidemic and zoonotic coronaviruses. Sci. Transl. Med. *9*, eaal3653. https://doi.org/10.1126/scitranslmed.aal3653.
39. Edwards, R.J., Mansouri, K., Stalls, V., Manne, K., Watts, B., Parks, R., Janowska, K., Gobeil, S.M.C., Kopp, M., Li, D., et al. (2021). Cold sensitivity of the SARS-CoV-2 spike ectodomain. Nat. Struct. Mol. Biol. *28*, 128–131. https://doi.org/10.1038/s41594-020-00547-5.
40. Scheres, S.H.W. (2016). Processing of Structurally Heterogeneous Cryo-EM Data in RELION. In Methods in Enzymology. The Resolution Revolution: Recent Advances in cryoEM, R.A. Crowther, ed. (Academic Press), pp. 125–157. https://doi.org/10.1016/bs.mie.2016.04.012.
41. Scheres, S.H.W. (2012). A Bayesian View on Cryo-EM Structure Determination. J. Mol. Biol. *415*, 406–418. https://doi.org/10.1016/j.jmb.2011.11.010.
42. Pettersen, E.F., Goddard, T.D., Huang, C.C., Couch, G.S., Greenblatt, D.M., Meng, E.C., and Ferrin, T.E. (2004). UCSF Chimera?A visualization system for exploratory research and analysis. J. Comput. Chem. *25*, 1605–1612. https://doi.org/10.1002/jcc.20084.
43. Goddard, T.D., Huang, C.C., Meng, E.C., Pettersen, E.F., Couch, G.S., Morris, J.H., and Ferrin, T.E. (2018). UCSF ChimeraX: Meeting modern challenges in visualization and analysis. Protein Sci. *27*, 14–25. https://doi.org/10.1002/pro.3235.
44. Dinnon, K.H., 3rd, Leist, S.R., Schäfer, A., Edwards, C.E., Martinez, D.R., Montgomery, S.A., West, A., Yount, B.L., Jr., Hou, Y.J., Adams, L.E., et al. (2020). A mouse-adapted model of SARS-CoV-2 to test COVID-19 countermeasures. Nature *586*, 560–566. https://doi.org/10.1038/s41586-020-2708-8.
45. Leist, S.R., Dinnon, K.H., 3rd, Schäfer, A., Tse, L.V., Okuda, K., Hou, Y.J., West, A., Edwards, C.E., Sanders, W., Fritch, E.J., et al. (2020). A Mouse-Adapted SARS-CoV-2 Induces Acute Lung Injury and Mortality in Standard Laboratory Mice. Cell *183*, 1070–1085.e12. https://doi.org/10.1016/j.cell.2020.09.050.
46. Wrapp, D., Wang, N., Corbett, K.S., Goldsmith, J.A., Hsieh, C.L., Abiona, O., Graham, B.S., and McLellan, J.S. (2020). Cryo-EM structure of the 2019-nCoV spike in the prefusion conformation. Science *367*, 1260–1263. https://doi.org/10.1126/science.abb2507.
47. Chen, L., Cohen, J., Song, X., Zhao, A., Ye, Z., Feulner, C.J., Doonan, P., Somers, W., Lin, L., and Chen, P.R. (2016). Improved variants of SrtA for site-specific conjugation on antibodies and proteins with high efficiency. Sci. Rep. *6*, 31899. https://doi.org/10.1038/srep31899.
48. Silva, J.C., Gorenstein, M.V., Li, G.Z., Vissers, J.P.C., and Geromanos, S.J. (2006). Absolute quantification of proteins by LCMSE: a virtue of parallel MS acquisition. Mol. Cell. Proteomics *5*, 144–156. https://doi.org/10.1074/mcp.M500230-MCP200.
49. Scobey, T., Yount, B.L., Sims, A.C., Donaldson, E.F., Agnihothram, S.S., Menachery, V.D., Graham, R.L., Swanstrom, J., Bove, P.F., Kim, J.D., et al. (2013). Reverse genetics with a full-length infectious cDNA of the Middle East respiratory syndrome coronavirus. Proc. Natl. Acad. Sci. USA. *110*, 16157–16162. https://doi.org/10.1073/pnas.1311542110.

STAR★METHODS

KEY RESOURCES TABLE

REAGENT or RESOURCE	SOURCE	IDENTIFIER
Antibodies		
Mouse-Anti-ST2 IgG	Invitrogen	Cat #MA5-37747; RRID:AB_2897671
Mouse-Anti-HisTag antibody His.H8	Invitrogen	Cat #MA1-21315; RRID:AB_557403
HRP goat anti-mouse IgG	SouthernBiotech	Cat #1030-05; RRID:AB_2619742
HRP goat anti-human IgG	SouthernBiotech	Cat #2040-05; RRID:AB_2795644
HRP goat anti-rabbit IgG	Abcam	Cat #ab97080; RRID:AB_10679808
Bacterial and virus strains		
SARS-CoV-2 virus, Isolate USA-WA1/2020	BEI Resources	Cat #NR-52281
SARS-CoV-2 nanoLuc virus	Hou et al.[37]	N/A
SARS-CoV nanoLuc virus	Sheahan et al.[38]	N/A
WIV1-CoV nanoLuc virus	Menachery et al.[20]	N/A
SARS-CoV mouse-adapted virus MA15	Roberts et al.[22]	N/A
MERS-CoV mouse-adapted virus m35c4	Douglas et al.[24]	N/A
Biological samples		
Plasma, nasal turbinates, and lungs from mice	This paper	N/A
Chemicals, peptides, and recombinant proteins		
SureBlue Reserve tetramethylbenzidine substrate	KPL	Cat #5120-0081
Luciferase Cell Culture Lysis 5x Reagent	Promega	Cat# E1531
Background Reducing Antibody Diluent	Agilent	Cat# S3022
PowerVision Poly-HRP anti-Rabbit IgG IHC Detection Systems	Leica	Cat# PV6121
Human ACE2 soluble protein	Edwards et al.[39]	N/A
SARS-CoV-2 Spike S2 ECD	This paper	N/A
SARS-CoV-2 Spike RBD	This paper	N/A
MERS-CoV Spike ECD	This paper	N/A
MERS-CoV Spike RBD	This paper	N/A
RsSHC014 Spike RBD	This paper	N/A
RsSHC014 Spike ECD	This paper	N/A
H. pylori Ferritin	This paper	N/A
Sortase A	This paper	N/A
CCoV-HuPn RBD	This paper	N/A
hCoV-OC43 RBD	This paper	N/A
WIV-1 RBD	This paper	N/A
SARS-CoV GZ02 RBD	This paper	N/A
BatCoV-ZC45 RBD	This paper	N/A
PCoV-GXP4L RBD	This paper	N/A
BatCoV-BANAL-236 RBD	This paper	N/A
BatCoV-NL140422 RBD	This paper	N/A
BatCoV-HKU4 RBD	This paper	N/A
BatCoV-HKU5 RBD	This paper	N/A
BatCoV-BtKY06 RBD	This paper	N/A
PdCoV-Haiti RBD	This paper	N/A

(*Continued on next page*)

Please cite this article in press as: Martinez et al., Vaccine-mediated protection against *Merbecovirus* and *Sarbecovirus* challenge in mice, Cell Reports (2023), https://doi.org/10.1016/j.celrep.2023.113248

Continued

REAGENT or RESOURCE	SOURCE	IDENTIFIER
Critical commercial assays		
Britelite Luminescence Reporter Gene Assay System	PerkinElmer Life Sciences	Cat #6066761
Nano-Glo Luciferase Assay System	Promega	Cat #N1150
Experimental models: Cell lines		
Vero E6	ATCC	Cat# CRL-1586
Freestyle 293F	ThermoFisher Scientific	Cat# R79007
Experimental models: Organisms/strains		
BALB/c mouse	Envigo	N/A
288/330 hDPP4 transgenic mice	Cockrell et al.[23]	N/A
Recombinant DNA		
HV1302284 (*H. pylori* Ferritin)	Saunders et al.[7]	N/A
HV1302277 (Sortase A)	Saunders et al.[7]	N/A
HV1302964 (SARS-CoV-2 RBD)	Saunders et al.[7]	N/A
HV1302315 (BatCoV-RsSHC014 RBD)	This paper	N/A
HV1301961_D614G (SARS-CoV-2 D614G S2P Spike)	This paper	N/A
HV1302109 (BatCoV-RsSHC014 S2P Spike)	This paper	N/A
HV1302103 (SARS-CoV Tor2 S2P Spike)	This paper	N/A
HV1302112 (MERS-CoV S2P Spike)	This paper	N/A
HV1302631 (CCoV-HuPn RBD)	This paper	N/A
HV1302784 (hCoV-OC43 RBD)	This paper	N/A
HV1302780 (WIV-1 RBD)	This paper	N/A
HV1302316 (SARS-CoV GZ02 RBD)	This paper	N/A
HV1303162 (BatCoV-ZC45 RBD)	This paper	N/A
HV1302314 (PCoV-GXP4L RBD)	This paper	N/A
HV1303029 (BatCoV-BANAL-236 RBD)	This paper	N/A
HV1302313 (MERS-CoV RBD)	This paper	N/A
HV1302782 (BatCoV-NL140422 RBD)	This paper	N/A
HV1303455 (BatCoV-HKU4 RBD)	This paper	N/A
HV1303456 (BatCoV-HKU5 RBD)	This paper	N/A
HV1303169 (BatCoV-BtKY06 RBD)	This paper	N/A
HV1302636 (PdCoV-Haiti RBD)	This paper	N/A
Software and algorithms		
GraphPad Prism v 9	GraphPad Software Inc	https://www.graphpad.com/scientific-software/prism/
PyMol	The PyMOL Molecular Graphics System (Schrödinger, 2015).	https://www.pymol.org/2/
SoftMax Pro	Molecular Devices	https://www.moleculardevices.com/
Adobe Illustrator 2020	Adobe	N/A
Relion	Scheres,[40] Scheres et al.[41]	Version 3.1
UCSF Chimera	Pettersen et al.[42]	http://www.cgl.ucsf.edu/chimera/
Chimera X	Goddard et al.[43]	https://www.rbvi.ucsf.edu/chimerax/
Adobe Photoshop CC 2019	Adobe	N/A

RESOURCE AVAILABILITY

Lead contact

Further information and requests for reagents should be directed and will be fulfilled by the Lead Contact David R. Martinez (david.martinez@yale.edu).

Materials availability

Reagents specific to this study are available from the Lead Contact with a completed Materials Transfer Agreement.

Data and code availability

- The data that support the findings of this study are available from the corresponding authors on request.
- This paper does not report original code.
- Any additional information required to reanalyze the data reported in this paper is available from the lead contact upon request.

EXPERIMENTAL MODEL AND STUDY PARTICIPANT DETAILS

Mouse models

Eleven to twelve-month old female immunocompetent BALB/c mice purchased from Envigo (BALB/c AnNHsd, stock# 047) were used for SARS-CoV-2 *in vivo* protection experiments as described previously.[44,45] 288/330-hDPP4 transgenic mice were bred and maintained at the University of North Carolina at Chapel Hill and used for MERS-CoV *in vivo* protection experiments. Mice were housed in groups of five animals per cage and fed standard chow diet. The study was carried out in accordance with the recommendations for care and use of animals by the Office of Laboratory Animal Welfare (OLAW), National Institutes of Health and the Institutional Animal Care. All mouse studies were performed at the University of North Carolina (Animal Welfare Assurance #A3410-01) using protocols (19–168) approved by the UNC Institutional Animal Care and Use Committee (IACUC) and all mouse studies were performed in a BSL3 facility at UNC.

METHOD DETAILS

Recombinant protein production

Recombinant viral proteins were produced in Freestyle293F cells by transient transfection as described previously.[15] Coronavirus proteins were cloned into pVRC8400 vector for mammalian expression. Plasmids were transiently transfected in FreeStyle 293F cells (Thermo Fisher) using ExpiFectamine (Thermo Fisher). The cultures were harvested on Day 6 post transfection, and protein was purified by StrepTactin resin (IBA) or HisTrap resin and size exclusive chromatography using Superose 6 or Superdex 200 column (GE Healthcare). Affinity tags were removed using HRV 3C protease (ThermoScientific) and the protein repurified using IMAC-Ni+ resin to remove the protease, tag and non-cleaved protein.

RBD SORTASE A CONJUGATED NANOPARTICLE VACCINE PRODUCTION

The receptor-binding domains (RBDs) from SARS-CoV-2 Wuhan-Hu1 isolate, MERS-CoV EMC isolate, and BatCoV RsSHC014 were expressed with a Sortase A donor sequence (LPETGG) encoded at the C terminus. An HRV-3C cleave site, an 8x His-tag, and a twin StrepTagII (IBA) were added C-terminal to the Sortase A donor sequence. The RBDs were each expressed by transient transfection using 293Fectin in Freestyle 293 cells and purified by StrepTactin affinity chromatography (IBA) followed by Superdex200 size-exclusion chromatography as described previously.[7,46] *Helicobacter pylori* ferritin particles were expressed with an N-terminal pentaglycine Sortase A acceptor sequence at the end of each subunit. 6x His-tags were included C-terminal to an HRV-3C cleavage site to enable affinity purification of the Ferritin particles. Prior to conjugation, RBDs, ferritin subunits, and pentamutant Sortase A[47] were buffer exchanged into 50mM Tris, 150mM NaCl, 5mM $CaCl_2$ at pH 7.4. The components were combined at a ratio of 360 μM total RBD (360 μM SARS-CoV-2 RBD for monovalent RBD scNP, or 120μM each of SARS-CoV-2, RsSHC014, and MERS-CoV RBD for the trivalent RBD scNP), plus 120μM Ferritin, plus 100μM Sortase A, and incubated at room temperature for 4 h. After incubation, the conjugated RBD-bearing nanoparticles were separated from free unconjugated reactants by size-exclusion chromatography using a Superose6 16/600 column. Conjugate nanoparticle assembly was confirmed by analytical size exclusion chromatography, NSEM, and Western blot under both reducing and non-reducing conditions.

LC-MS/MS proteomics analysis

Samples were brought to 4% SDS in 20 mM Tris and were spiked with 1pmol bovine alpha casein as an internal digestion control. Samples were then reduced with 10 mM dithiolthreitol for 20 min at 55C, subjected to three rounds of batch sonication at 30% power, alkylated with 25mM iodoacetamide for 45 min at room temperature and then subjected to S-trap (Protifi) trypsin digestion using manufacturer recommended protocols. Digested peptides were lyophilized to dryness and resuspended in 0.2% formic acid/2%

acetonitrile. Each sample was subjected to chromatographic separation on a Waters MClass UPLC equipped with a 1.8 μm Acquity HSS T3 C18 75 μm × 250 mm column (Waters Corp.) with a 90-min linear gradient of 5–30% acetonitrile with 0.1% formic acid at a flow rate of 400 nL/min (nL/min) with a column temperature of 55°C. Data collection on the Fusion Lumos mass spectrometer was performed for three difference compensation voltages (−40v, −60v, −80v). Within each CV, a data-dependent acquisition (DDA) mode of acquisition with an r = 120,000 (@ m/z 200) full MS scan from m/z 375–1500 with a target AGC value of 4e5 ions was performed. MS/MS scans with HCD settings of 30% were acquired in the linear ion trap in "rapid" mode with a target AGC value of 1e4 and max fill time of 35 ms. The total cycle time for each CV was 0.66s, with total cycle times of 2 s between like full MS scans. A 20s dynamic exclusion was employed to increase depth of coverage. The total analysis cycle time for each sample injection was approximately 2 h.

Raw LC-MS/MS data files were processed in Proteome Discoverer 3.0 (Thermo Scientific) and individual LCMS data files were aligned based on the accurate mass and retention time of detected precursor ions ("features") using Minora Feature Detector algorithm. Relative peptide abundance was measured based on peak intensities of selected ion chromatograms of the aligned features across all runs. The MS/MS data was searched against the SwissProt H. sapiens database containing custom RBD and Ferritin sequences, a common contaminant/spiked protein database (bovine albumin, bovine casein, yeast ADH, etc.), and an equal number of reversed-sequence "decoys" for false discovery rate determination. Sequest was utilized to produce fragment ion spectra and to perform the database searches. Database search parameters included fixed modification on Cys (carbamidomethyl) and variable modification on Met (oxidation). Search tolerances were 2ppm precursor and 0.8 Da product ion with full trypsin enzyme rules. Peptide Validator and Protein FDR Validator nodes in Proteome Discoverer were used to annotate the data at a maximum 1% protein false discovery rate based on q-value calculations. Following LFQ quantitation, total signal was normalized across all three replicates and then the average intensity of the top three most abundant peptides for each of the proteins of interest was used for stoichiometry measurements.[48]

Biolayer interferometry (BLI)

Antibody binding was determined using a FortéBio Bio-Layer Interferometry instrument (Sartorius Octet Red96e) at 25°C with a shake speed of 1000 rpm. Antibodies were diluted to 20 μg/mL in a flat bottom 96-well plate (Greiner) with 0.22 μm filtered phosphate buffered saline pH 7.4 and 0.05% Tween 20 (PBS-T). The antigens were diluted to a concentration of 50 μg/mL using PBS-T. Hydrated Anti-hIgG Fc Capture (AHC) biosensors (Sartorius #18–5060) were equilibrated for 60 s and then antibodies were loaded to biosensors for 300 s. After a 60-s wash and a 180-s baseline step, biosensors were then dipped into the diluted antigens for a 200-s association. Next, antibody and antigens allowed to dissociate for 300 s. Data was analyzed using Data Analysis HT 12.0 software. The negative control antibody, CH65, was indicated as a reference sensor and subtracted from the remaining ligand sensor measurements. Data was then aligned to the average of the baseline step and plotted using GraphPad Prism 9 software.

Negative stain electron microscopy of RBD nanoparticles

Negative stain electron microscopy was performed as previously described.[7] The RBD nanoparticle protein was thawed in an aluminum block at room temperature for 5 min. The RBD scNP was diluted to a final concentration of 0.2 mg/mL into room temperature buffer containing 150 mM NaCl, 20 mM HEPES pH 7.4, 5 g/dL glycerol and 8 mM glutaraldehyde. After 5 min, the cross-linking was quenched by the addition of 1 M Tris pH 7.4 to a final concentration of 75 mM Tris and incubated for 5 min. Carbon-coated grids (EMS, CF300-cu-UL) were glow-discharged for 20 s at 15 mA, and subsequently a 5-μL drop of quenched sample was incubated on the grid for 10–15 s. The grid was blotted and then stained with 2 g/dL uranyl formate. After air drying, grids were imaged with a Philips EM420 electron microscope operated at 120 kV, at 49,000× magnification and images captured with a 76 megapixel CCD camera at a pixel size of 2.4 Å.

Processing of negative-stain images

The RELION 3.0 program was used for all negative-stain image processing following previously published procedures.[7] Images were CTF-corrected with CTFFIND and particles were picked using a nanoparticle template. Extracted particle stacks were underwent 2 or 3 rounds of 2D class averaging and selection to discard irrelevant particles and background picks.

Mouse vaccinations and virus challenge experiments

Aged BALB/c (#047) retired breeder female mice were purchased from Envigo and were used for SARS-CoV MA15 challenge studies. B6 male and female mice modified at the DPP4 locus[23] to allow pathogenesis by mouse-adapted MERS-CoV m35c4[24] were bred in house and used at ~20–25 weeks of age. Group sizes ranged from 9 to 16 mice such that a minimum of five mice would be available for immunologic and virologic assessment at different timepoints. One study had 6 mice harvested at the peak lung virus replication timepoint and 3 mice were kept for longer follow up at a second timepoint. Five mice or greater was chosen as the target number, since that is the lowest number of mice within a group that can be compared at two different timepoints with a two-tailed nonparametric test and reach statistical significance. The Toll-like receptor 4 agonist glucopyranosyl lipid adjuvant–stable emulsion (GLA-SE) was used as the adjuvant for the vaccine immunogens. Mouse vaccination studies were performed intramuscularly with GLA-SE-adjuvanted SARS-CoV-2 RBD scNP, GLA-SE-adjuvanted SARS-CoV-2/RsSHC014/MERS-CoV RBD scNP, or GLA-SE-adjuvant only for the control group. Vaccine immunogens were administered at 10 μg of the RBD scNP vaccines formulated with 5 μg of adjuvant.

Mice were immunized at week 0 and week 4 for the 2X prime-boost vaccine regimen, and at week 0, week 4, and week 8 for the 3X prime-boost-boost vaccine regimen. Mice were then moved into the BSL3 and acclimated for a few days. Prior to challenge, mice were anesthetized with an intraperitoneal delivery of xylazine and ketamine and given a lethal dose of SARS-CoV MA15[22]: 1×10^4 PFU/mL. For the MERS-CoV challenge studies, mice were challenged with mouse-adapted MERS-CoV m35c4.[24]

Binding ELISA against coronavirus antigen panel

For coronavirus antigen-binding assays, 384-well ELISA plates (Costar #3700) were coated with 2 μg/mL antigens in 0.1M sodium bicarbonate overnight at 4°C. Plates were then washed 1X and blocked for 2 h at room temperature with SuperBlock (1X phosphate buffered saline (PBS) containing 4% (w/v) whey protein 15% normal goat serum/0.5% Tween 20/0.05% sodium azide). Mouse serum samples were collected at baseline before prime, two weeks post prime, four weeks post prime, two weeks post boost, and two weeks post the second boost. Mouse serum samples were added at 1:30 dilution in SuperBlock and diluted 3-fold through 12 dilution spots to generate binding curves. Diluted serum samples were bound to coated plates in SuperBlock for 1h at room temperature. Plates were then washed 2X and a horseradish peroxidase (HRP)-conjugated goat anti-mouse IgG secondary antibody (SouthernBiotech 1030-05) was added in SuperBlock at a 1:16,000 dilution. Secondary antibody was bound for 1h and then washed 4X and detected with 20μL SureBlue Reserve (KPL 53-00-03) for 15 min. Colorimetric reactions were stopped by adding 20μL of 1% HCL stop solution. Plates were read at 450nm and area under the curve (AUC) was calculated from the serially diluted mouse serum samples.

ACE2-blocking and DPP4-blocking assays

Blocking assays were performed by ELISA as stated previously.[15] Plates were coated with ACE2 or DPP4 as stated above at 2 μg/mL. In a separate dilution plate Spike-2P protein was mixed with a 1:30 dilution of serum at a final concentration equal to the EC50 at which spike binds to its receptor protein. The Spike and antibody solution was added the receptor to determine binding. The magnitude of Ab blocking of the binding of spike protein to its receptor was determined by comparing the optical density (OD) at 450 nm of Ab plus spike to the OD of wells containing spike protein without Ab. The formula below was used to calculate percent blocking: blocking% = (100 - (OD Ab+spike/OD of spike only)*100) as stated previously.[15]

Live virus neutralization assays

All live virus assays were performed in a BSL-3 laboratory. Full length SARS-CoV Urbani, WIV-1, SARS-CoV-2 Wuhan-1 expressing the BA.1 spike, SARS-CoV-2 Wuhan-1 expressing the XBB1.5 spike, and MERS-CoV were designed to express nanoluciferase (nLuc) as described previously.[37,49] SARS-CoV Urbani, SARS-CoV-2 BA.1, SARS-CoV-2 XBB.1.5, and WIV-1 stocks were generated and titrated in Vero E6 (C1008) cells and MERS-CoV stocks were titrated in Vero 81 (CCL-81) cells. For the live virus neutralization assays, cells were plated at 20,000 cells per well in clear bottom, black-walled 96-well plates the day prior to the assay. On the day of the assay, mouse serum samples diluted 1:40 and serially diluted 3-fold to eight dilutions. Serially diluted mouse serum was added at a 1:1 volume with diluted virus and incubated for 1 h. Antibody-virus dilutions were then added to cells at 800 PFU per well and incubated at 37°C with 5% CO_2. Following a 24h incubation, plates were read by adding 25μL of Nano-Glo Luciferase Assay System (Promega). Luminescence was measured by a Spectramax M3 plate reader (Molecular Devices). Fifty percent virus neutralization titers were calculated using GraphPad Prism via four-parameter dose-response curves.

Biocontainment and biosafety

All experiments handling live viruses, including mouse-adapted coronaviruses, were performed in an animal biosafety level 3 (BSL-3) laboratory. Laboratory workers performing BSL-3 experiments wore powered air purifying respirators (PAPR), Tyvek coverall suits, double booties covering footwear, and double gloves. All recombinant coronavirus work was approved by the UNC Institutional Biosafety Committee (IBC). All animal work was approved by the UNC Institutional Animal Care and Use Committee (IACUC). All BSL-3 work was performed in a facility conforming to requirements recommended in the Microbiological and Biomedical Laboratories, by the U.S. Department of Health and Human Services, the U.S. Public Health Service, and the U.S. Center for Disease Control and Prevention (CDC), and the National Institutes of Health (NIH).

QUANTIFICATION AND STATISTICAL ANALYSIS

Non-parametric Kruskal-Wallis tests were used to compare lung and nasal turbinate infectious virus replication in challenged mice and neutralizing antibody assays. A Dunn's test was used to correct for multiple comparisons. A Chi square log rank test was used for the survival analysis. Statistical analyses were performed in GraphPad Prism 9.